

Online Load and Leakage Estimation in Hydraulic Pitch System for Wind Turbines

C. S. Pedersen M. Fink M. Bhola H. C. Pedersen

Abstract

In wind turbines, the pitch system is a critical subsystem for both regulating the power output and for the safety of the turbine. However, it is also one of the leading contributors to downtime in turbines, as it is prone to faults like internal and external leakage. In this article, a novel method for estimating load and leakage in hydraulic pitch systems is presented. The proposed method is based on Unscented Kalman Filters, where the method integrates load estimation to handle the stochastic nature of wind loads, enhancing the accuracy of leakage detection. Based on the developed method, simulation and experimental results are presented that demonstrate the feasibility and robustness of the method under varying operating conditions and for different parameter variations. From the results, it is therefore found that the method shows good promise for being applied in condition monitoring and fault detection in pitch systems and may therefore be used to reduce downtime and maintenance costs in wind turbine operations.

Keywords: Unscented Kalman Filter, Online Estimation, Load Estimation, Leakage Estimation, Wind Turbine Pitch System

1 Introduction

The pitch system is a critical subsystem in wind turbines, responsible for regulating power output above rated wind speeds and acting as an aerodynamic brake during emergency shutdowns. As highlighted by Padman et al. (2016), pitch system failures are the leading contributor to wind turbine downtime, resulting in substantial economic losses due to interrupted energy production. A recent reliability analysis by Walgern et al. (2023) examined hydraulic and electrical pitch systems over 1847 and 848 operational years, respectively, and concluded that hydraulic systems exhibit slightly higher reliability, with 0.54 failures per turbine per year, compared to 0.56 for electrical systems. In efforts to reduce the Levelized Cost of Energy (LCoE), the wind energy sector is moving towards larger turbine sizes. Shields et al. (2021) demonstrated that for turbines ranging from 6-20 MW and wind plants of 250–2500 MW, larger turbine sizes can reduce LCoE by up to 23%. This upscaling trend results in longer and heavier blades, for which hydraulic pitch systems are particularly well-suited due to their high power-to-weight ratio, scalability, and intrinsic shockabsorbing properties Lu et al. (2009); Palanimuthu and Joo (2023).

Faults within hydraulic pitch systems vary in severity. Dallabona et al. (2025) classify these into high, medium, and low categories. High-severity faults may thus include both external and internal leakage in valves and cylinders, as well as friction increases in actuators and rotary-union bearings. Accurate estimation of leakage and load based on existing sensor data is thus essential for implementing e.g. fault-tolerant control strategies and for predicting wear-related failures and remaining useful life (RUL) of system components.

Leakage estimation has been extensively studied, with existing methods broadly categorized as either

¹Department of Energy Technology, Aalborg University, Pontoppidanstraede 111, 9220 Aalborg, Denmark. E-mail: {cspe, mfin, mobh, hcp}@energy.aau.dk

model-based or data-driven. Model-based approaches commonly utilize a Kalman filter-type approach to estimate leakage directly or through leakage coefficients. Data-driven methods, on the other hand, extract features from sensor data collected under various operational conditions and use machine learning models to classify fault levels, typically through offline, post-processing workflows. However, for systems subjected to stochastic loading conditions such as wind turbines, data-driven models require large, high-quality datasets, which limits their practicality. As a result, leakage detection methods using data-driven approaches have almost entirely focused on applications with known load characteristics.

A combined Wavelet Packet Transformation (WPT) and Support Vector Machine (SVM) method was proposed by Ma et al. (2023) for leakage detection in hydraulic cylinders used in marine systems. Their methodology, validated against AMESim-based simulations and experimental data, involved frequency-domain analysis of pressure signals and SVM-based fault classification. However, the approach is limited by its reliance on simplified loading conditions. Other WPT-based studies Zhao et al. (2015); Na et al. (2022) have also shown promising results in fault classification by correlating energy features with known fault levels. Nonetheless, they typically do not account for external disturbances such as fluctuating wind loads, which could be addressed through load estimation.

In a more application-specific context, Wu et al. (2012) presented an adaptive parameter estimation method to identify both internal and external leakage, using wind load data from the NREL 1.5 MW Open-FAST model. Experimental validation on a scaled laboratory setup showed promising results, though the method relied on flow-rate sensors that are rarely used in full-scale turbines due to cost. Similarly, Choux et al. (2012) used residual analysis and multiple Extended Kalman Filters (EKFs) to detect leakage by comparing estimated and measured system behavior. Their approach included modeling different leakage scenarios—ranging from zero to combined internal and external leakage—and emphasized the need for a reliable fault-free reference model. While both EKF and State-Augmented EKF (SAEKF) techniques proved effective, SAEKF was found to be significantly more computationally demanding, requiring up to twelve times more resources, and both approaches needed sampling rates of at least 1 kHz to be effective. Moreover, the experimental setup did not fully replicate real turbine loading conditions, raising concerns about realworld applicability.

In addition to leakage, increasing cylinder friction may also be monitored for predicting faults related to worn-out seals and metal-to-metal contact. Márton et al. (2011) employed a piecewise linear approximation technique to identify friction parameters for linear actuators but using bang-bang control inputs to the servo valve. Data from pressure sensors and velocity measurements were utilized to estimate the friction parameter. However, the impact of oil temperature on the friction parameter was not addressed. Nonetheless, the method could be applied for online monitoring of friction force in hydraulic cylinders in operations, potentially serving as a fault identification metric as cylinder wear increases, but its applicability is limited to applications with a constant or known load force. For real-time condition monitoring in wind turbines, Dallabona et al. (2024) proposed a method for detecting friction-related faults using wear-sensitive friction modeling. By incorporating a root-bending moment sensor and applying a sliding mode robust differentiator with band-stop filtering, the approach isolated friction effects from wind-induced disturbances. A modified least squares estimator was then used to ensure convergence and enable statistical change detection, thereby minimizing false alarms during operation. However, despite the method showed promising results, installing a root-bending torque sensor will not be a feasible approach for most wind turbine applications.

As apparent from the above, research related to leakage estimation in hydraulic cylinders is typically linked to a constant or known loading of the cylinder. In reality, the load force on the pitch cylinder is composed of both gravitational forces from the blade, blade dvnamics, and unknown and stochastic loading from the wind. Therefore, the focus of the current article is on leakage estimation in hydraulic pitch systems, but taking into account the unknown variations in the wind loads. Specifically the article investigates and presents a method for internal leakage detection in hydraulic pitch system, i.e. the cylinder and proportional valve, as this is shown to degrade the performance of the pitch position controller. However, the method is applicable to external leakage as well, but the two types of leakage cannot be separated from each other with the presented method, and with the used experimental setup it is only possible to test for internal leakage. As the focus is on wind turbines with stochastic loads, the approach is based on a model-based approach using an Unscented Kalman Filter, but also incorporating a load estimation algorithm for handling the unknown loading of the cylinder. The presented methods thus contains both a load estimation scheme that may be utilized separately, and a leakage estimation scheme, and the two methods are tested in both simulation and experimentally on a full scale pitch system set-up, where real wind conditions are emulated. Based on these results, it is shown that the methods accurately estimate both the internal leakage and the load torque in the system, while both methods also exhibit robustness to parameter uncertainties and unknown wind conditions.

The paper is organized as follows: In section two, the system is described along with a model. In section three, the load estimation algorithm is presented, and in section four, the leakage estimation method is presented. In section five, simulation results are presented, also showing the robustness towards parameter variations. In section six, the experimental set-up is presented along with the experimental results validating the algorithms, and finally, in section seven, the conclusions are presented.

2 System Description and Model

The model of the turbine is based on the NREL 5MW turbine and utilizing OpenFAST, where the system has been modified to include a hydraulic pitch system. The latter is based on a standard state of the art configuration and designed/scaled to the 5MW turbine. The model for the simplified hydraulic pitch system is presented in the following, where the model is based on experimentally validated models of a similar pitch system. The pitch system centers around a disk that connects the turbine blade to the rotor hub through the blade bearing. The bearing disk is actuated by the hydraulic cylinder (C1 in Figure 1), that actuates the disk at an angle, to change the blade pitch. The pitch system is powered by a Hydraulic Power Unit (HPU) in the turbine nacelle, connected through a hydraulic rotary union (R1).

A diagram of the main parts of the hydraulic system can be seen in Figure 1.

2.1 Model

In the following, the model of the pitch system is presented, including a model of the proportional valve, and the mechanical connection to the blade.

2.1.1 Hydraulic Model

The hydraulics of the pitch system are modeled using a lumped parameter model. A diagram of the hydraulic system is shown in Figure 2. The hydraulic system is divided into two control volumes: the piston (p_p) and rod (p_r) sides of the pitch cylinder, whereas the supply pressure is assumed constant without loss of generality. Pressure gradients for each volume are modelled using

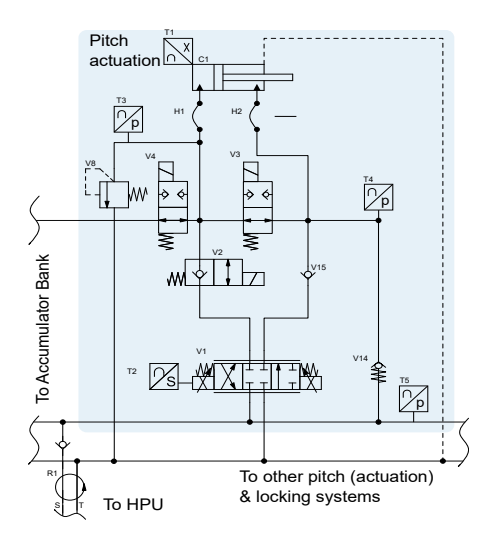


Figure 1: Hydraulic diagram of the main parts of a turbine pitch system. Valves V2, V3 and V4 make op the emergency pitch system. These valves are shown in their OFF state, during normal operation they are turned ON.

the continuity equation, as:

$$\dot{p}_p = \frac{\beta_p}{V_p} \left(Q_p + Q_{le} - A_p \dot{x}_p \right) \tag{1}$$

$$\dot{p}_r = \frac{\beta_r}{V_r} \left(A_r \dot{x}_p - Q_r - Q_{le} \right) \tag{2}$$

where β_i is the oil bulk modulus of the respective chamber, which is modelled as being pressure and air dependent, and V_i is the volume of the respective chamber, which is a function of the piston position. The flows across the proportional valve are modelled using the orifice equation, with the modification that positive Q_T

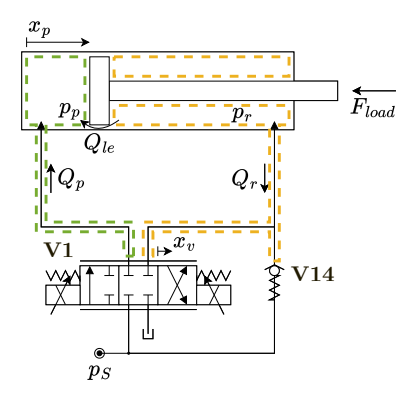


Figure 2: Hydraulic model diagram. Valves **V2**, **V3** and **V4** are modelled in their ON state, valve **V15** is neglected.

flow is going across the check valve, thus:

$$Q_{p} = H(x_{v})C_{d}A(x_{v})\sqrt{\frac{2}{\rho}|p_{s}-p_{p}|}\operatorname{sign}(p_{s}-p_{p})$$
(3)
+ $H(-x_{v})C_{d}A(x_{v})\sqrt{\frac{2}{\rho}|p_{p}-p_{t}|}\operatorname{sign}(p_{p}-p_{t})$ (4)

$$Q_r = H(-x_v)C_dA(x_v)\sqrt{\frac{2}{\rho}|p_s - p_r|}\operatorname{sign}(p_s - p_r) \quad (5)$$

$$+H(x_v)K_c(p_r-p_s-p_{cr}) \tag{6}$$

where $H(\cdot)$ is the Heaviside function, $A(x_v)$ is the respective opening area of the valve, C_d the discharge coefficient, and K_c and p_{cr} are respectively the flow coefficient and crack pressure for the check valve. Finally, the leakage flow (Q_{le}) is assumed laminar, thus yielding the model:

$$Q_{le} = C_{le} \left(p_r - p_p \right) \tag{7}$$

where C_{le} is the leakage coefficient. For the 4/3 proportional valve the area characteristic of the valve is approximated from available data. The movement dynamics of the valve is approximated as a 2nd order system and including a slew rate limitation.

2.1.2 Mechanical Model

A kinematic diagram of the pitch system can be seen in Figure 3. Here θ_p is the pitch angle, which varies in the

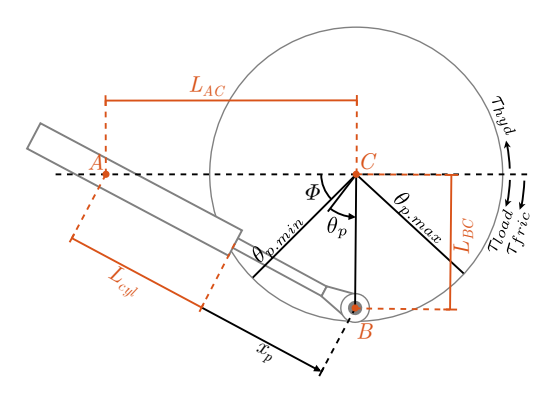


Figure 3: Simplified diagram of the turbine pitch system.

range -3° to 87° , with the blade fully out of the wind at $\theta_p = 87^{\circ}$, and fully into the wind at $\theta_p = 0^{\circ}$. A is the hinge point around which the pitch cylinder rotates, B is the point where the pitch cylinder connects to the bearing disk, and C is the center of the bearing disk. Since the pitch cylinder is linked to the bearing disk, extension of the pitch cylinder, x_p , is uniquely related to the pitch angle θ_p as:

$$x_p(\theta_p) = \sqrt{L_{AC}^2 + L_{BC}^2 - 2L_{AC}L_{BC}\cos(\Phi + \theta_p + \theta_{off})}$$
$$-L_{cyl}$$
(8)

By which the Drive Jacobian can be defined as:

$$\mathcal{J}(\theta_p) = \frac{\partial x_p}{\partial \theta_p}, \qquad \dot{x}_p = \mathcal{J}(\theta_p) \cdot \dot{\theta}_p \qquad (9)$$

By assuming no power loss in the gearing between x_p and θ_0 , the cylinder torque on the bearing disk can also be found using the Drive Jacobian:

$$\tau_{hyd} = \mathcal{J}(\theta_p)^T \cdot F_{hyd} \tag{10}$$

Dynamics

To model the dynamics of the mechanical part of the turbine pitch system the Euler-Lagrange equation is used, where the pitch angle θ_p is chosen as the generalized coordinate. The external torque includes the torque exerted by the hydraulic pitch cylinder, the load torque exerted by the wind, and friction torques:

$$\tau_{ext} = \tau_{hyd} - \tau_{fric} - \tau_{load} \tag{11}$$

The friction torque is modelled as viscous and Coulomb friction, with the tangent hyperbolic function replacing the sign function to avoid numerical problems:

$$\tau_{fric} = B_v \cdot \dot{\theta}_p + \tau_{Coulomb} \cdot \tanh\left(K_{tanh} \cdot \dot{\theta}_p\right) \quad (12)$$

where B_v and $\tau_{Coulomb}$ are combined values for the cylinder and bearing disk, and K_{tanh} is a constant that adjusts the hyperbolic tangent curve.

The variation in potential energy is zero, why the Lagrangian of the mechanical turbine pitch system can be described from the kinetic energy only. The mechanical dynamics is then derived from the Euler Lagrange equations as:

$$\ddot{\theta}_p = \frac{\tau_{ext} - m_p \mathcal{J}(\theta_p) \dot{\mathcal{J}}(\theta_p) \dot{\theta}_p^2}{m_p \mathcal{J}(\theta_p)^2 + J_b}$$
(13)

where m_p is mass of the pitch cylinder, J_b is the inertia of the bearing disk. Further, the rotational kinetic energy of the pitch cylinder is neglected, as the rotational speed and inertia of the cylinder is found to be significantly smaller than that of the blade and bearing disk.

3 Load Estimation using Unscented Kalman Filter

As described in the introduction, most leakage estimation methods rely on a well-known or repetitive load in the system. However, for wind turbines the pitch load is unknown and stochastic, why in the following, an Unscented Kalman Filter (UKF) is developed to estimate the load on the pitch cylinder. An UKF approach is here used as opposed to the more widely

used Extended Kalman Filter (EKF), due to the highly non-linear nature of the hydraulic pitch system and the stochastic nature of the wind load. Comparing the two different Kalman filter approaches (Wan and van der Merwe, 2001), the UKF is based on the unscented transform, which is second order accurate, whereas the EKF only provides first order accuracy. Furthermore, the EKF algorithm requires heavy computational effort, as the Jacobian of the non-linear system needs to be found analytically or using a numerical method.

3.1 UKF algorithm

As mentioned, the UKF is based on the unscented transform, first described in (Julier and Uhlmann, 1997). Calculating a set of σ -points, the unscented transform captures the true mean and covariance of a nonlinear system by propagating them through the nonlinear system equations directly. Therefore, for highly non-linear systems as the hydraulic pitch system, the UKF is expected to have an increased performance compared to the standard EKF.

The UKF algorithm requires that the state estimation vector, $\hat{\mathbf{x}}$, and the state estimation error covariance matrix, \mathbf{P} , are estimated at the first time step to initialize the filter. This is done as:

$$\hat{\mathbf{x}}_0 = E\left(\mathbf{x}_0\right) = E\left(\left[\theta_p \ \dot{\theta}_p \ p_p \ p_r\right]^T\right) \tag{14}$$

$$\mathbf{P}_0 = E\left(\left(\mathbf{x}_0 - \hat{\mathbf{x}}_0 \right) \left(\mathbf{x}_0 - \hat{\mathbf{x}}_0 \right)^T \right) \tag{15}$$

where E denotes the expected value of the state, which in this case is the initial value of the state. Typically, the initial states are not known and, therefore, the initial states are estimated with a best guess to initialize the filter. The UKF algorithm is divided into two subsections, the prediction step and the correction step, as described next.

3.1.1 Prediction step

The prediction step uses the state estimation vector and the state estimation error covariance matrix from the last time step to update them at the current time step. This is done by calculating a set of σ -points of which the weighted mean and covariance matrices are determined in order to calculate the Kalman gain.

Equation (16) calculates the σ -point matrix, where each vector in the matrix corresponds to a set of σ -points in the state space:

$$\hat{\mathbf{x}}_{k|k-1}^{(0)} = \hat{\mathbf{x}}_{k|k-1}
\hat{\mathbf{x}}_{k|k-1}^{(i)} = \hat{\mathbf{x}}_{k|k-1} + \Delta \mathbf{x}^{(i)}$$
(16)

 $\Delta \mathbf{x}^{(i)}$ determines the spread of the σ -points and is determined as:

$$\Delta \mathbf{x}^{(i)} = \left(\sqrt{c\mathbf{P}_{k|k-1}}\right)_{i}, \ i = 1, 2, ..., M$$
$$\Delta \mathbf{x}^{(M+i)} = -1 \cdot \left(\sqrt{c\mathbf{P}_{k|k-1}}\right)_{i}, \ i = 1, 2, ..., M$$

where $c = \alpha^2 (M + \kappa)$, with α and κ being parameters that determine the spread of the σ -points, and M is the number of states in the system. Further, the matrix square root is calculated using the Cholesky factorization using the lower triangle of the state estimation error covariance matrix.

Extracting the σ points from the measured states, the weighted mean, covariance, and cross covariance are determined as:

$$\hat{\mathbf{y}}_{k|k-1}^{(i)} = \mathbf{C} \cdot \hat{\mathbf{x}}_{k|k-1}^{(i)}, \ i = 0, 1, 2, ..., M$$
 (17)

$$\hat{\mathbf{y}}_k = \sum_{i=0}^{2M} \left(W_M^{(i)} \cdot \hat{\mathbf{y}}_{k|k-1}^{(i)} \right)$$
 (18)

$$\mathbf{P}_{Y} = \sum_{i=0}^{2M} W_{C}^{(i)} \left(\hat{\mathbf{y}}_{k|k-1}^{(i)} - \hat{\mathbf{y}}_{k} \right) \left(\hat{\mathbf{y}}_{k|k-1}^{(i)} - \hat{\mathbf{y}}_{k} \right)^{T} + R_{k}$$
(19)

$$\mathbf{P}_{XY} = \frac{1}{2\alpha^2 (M+\kappa)} \cdot \sum_{i=1}^{2M} \left(\hat{\mathbf{x}}_{k|k-1}^{(i)} - \hat{\mathbf{x}}_{k|k-1} \right) \left(\hat{\mathbf{y}}_{k|k-1}^{(i)} - \hat{\mathbf{y}}_k \right)^T \quad (20)$$

where **C** is the system output matrix, $\mathbf{R_k}$ is the measurement noise covariance matrix and the weights $W_M^{(i)}$ and $W_C^{(i)}$ are given as:

$$W_M^{(0)} = 1 - \frac{M}{\alpha^2 (M + \kappa)} \tag{21}$$

$$W_M^{(i)} = \frac{1}{2\alpha^2 (M + \kappa)}, i = 1, 2, ..., 2M$$
 (22)

$$W_C^{(0)} = (2 - \alpha^2 + \beta) - \frac{M}{\alpha^2 (M + \kappa)}$$
 (23)

$$W_{C}^{(i)} = \frac{1}{2\alpha^{2} (M + \kappa)} , i = 1, 2, ..., 2M$$
 (24)

where β is a parameter that adjusts the assumed distribution. The estimate of the system states and the state estimation error covariance matrix are obtained

$$\mathbf{K} = \mathbf{P}_{XY} \cdot \mathbf{P}_{Y}^{-1} \tag{25}$$

$$\hat{\mathbf{x}}_{k|k} = \hat{\mathbf{x}}_{k|k-1} + \mathbf{K} \left(\mathbf{y}_k - \hat{\mathbf{y}}_k \right) \tag{26}$$

$$\mathbf{P}_{k|k} = \mathbf{P}_{k|k-1} - \mathbf{K} \cdot \mathbf{P}_Y \cdot \mathbf{K}^T \tag{27}$$

Where \mathbf{K} is the Kalman gain.

3.1.2 Correction step

Estimates of the state estimation vector and state estimation error covariance matrix at the next time step are found by calculating a new set of σ -points as:

$$\hat{\mathbf{x}}_{k|k}^{(0)} = \hat{\mathbf{x}}_{k|k}$$

$$\hat{\mathbf{x}}_{k|k}^{(i)} = \hat{\mathbf{x}}_{k|k} + \Delta \mathbf{x}^{(i)}$$
(28)

and propagating each σ -point through the non-linear state transition function using the Forward-Euler method to predict the state vector as:

$$\hat{\mathbf{x}}_{k+1|k}^{(i)} = \mathbf{f}\left(\hat{\mathbf{x}}_{k|k}^{(i)}, u_k\right) \cdot T_s + \hat{\mathbf{x}}_{k|k}^{(i)} \tag{29}$$

where u_k is the input to the system, T_s is the sample time, and $\mathbf{f}(\hat{\mathbf{x}}_{k|k}^{(i)}, u_k)$ is the non-linear state transition

A weighted mean of the state estimation vector and the state estimation error covariance is found to update the algorithm for the next time step:

$$\hat{\mathbf{x}}_{k+1|k} = \sum_{i=0}^{2M} W_M^{(i)} \hat{\mathbf{x}}_{k+1|k}^{(i)}$$
(30)

$$\mathbf{P}_{k+1|k} = \sum_{i=0}^{2M} W_C^{(i)} \left(\hat{\mathbf{x}}_{k+1|k}^{(i)} - \hat{\mathbf{x}}_{k+1|k} \right) \left(\hat{\mathbf{x}}_{k+1|k}^{(i)} - \hat{\mathbf{x}}_{k+1|k} \right)^T + \mathbf{Q}_k$$
(31)

where \mathbf{Q}_k is the process noise covariance matrix.

3.1.3 Scaling

Hydraulic systems are known to be numerically badly scaled due to the numerically large pressures compared to angular position and velocity. Therefore, to avoid any computational issues when calculating the Cholesky decomposition, the state vector of the UKF is scaled such that all numerical values are within a reasonable region. Therefore, since the maximum system pressure of the HPU is 210 bar, the pressure states are scaled by the inverse of this. The position and velocity states are not scaled as their respective numerical values are within a region of which numerical issues are not a problem.

3.1.4 Adjusting Parameters

The UKF is adjusted through three tunable parameters $(\alpha, \beta \text{ and } \kappa)$, and the system specific process noise, \mathbf{Q}_k , measurement noise, \mathbf{R}_k , and covariance matrices.

The α parameter adjusts the spread of the σ -points and is usually chosen between 1 and 0, and κ is a secondary spread parameter to adjust σ -point spread (Wan and van der Merwe, 2001), but is often set to zero, (Simon, 2006; Van Der Merwe and Wan, 2001), which is also the case used here. Finally, as the distribution is assumed Gaussian $\beta = 2$ is used for the load estimation.

From the initial adjustments for the UKF parameters for the leakage estimator, it is found that a β value of 1.2 gives a good result. This suggests that the state covariance distribution of the pitch system is not Gaussian.

The process noise covariance matrix \mathbf{Q}_k describes how much the model from the state transition function is trusted, how much inaccuracy there is in the model, and how much external disturbance there is. If a value in \mathbf{Q}_k is decreased the Kalman filter will rely more on the model and less on measurements for the given state, and vice versa. The measurement noise covariance matrix \mathbf{R}_k describes how much noise there is in the measured signals. In this project \mathbf{Q}_k and \mathbf{R}_k are assumed to be diagonal matrices, meaning that process and measurement noise is not correlated between

The tuning of Q_k was initially based on an analysis of the system's sensitivity to noise and the amplitude of the load. However, this initial approach did not lead to stable estimation. Instead, it served as a starting point for a trial-and-error-based adjustment process, which led to the following set of parameter sets used in the final implementation for the leakage estimator:

$$\mathbf{R}_{k_{\text{BLLG}}} = \begin{bmatrix} 0.1 & 0.1 & 0.1 & 0.1 \end{bmatrix} \tag{32}$$

$$\mathbf{R}_{k_{DIAG}} = \begin{bmatrix} 0.1 & 0.1 & 0.1 & 0.1 \end{bmatrix}$$
 (32)
$$\mathbf{Q}_{k_{DIAG}} = \begin{bmatrix} 10^{-4} & 10^{-2} & 10^{-6} & 10^{-4} & 10^{-3} \end{bmatrix}$$
 (33)

$$\alpha = 10^{-4} \land \beta = 1.2 \tag{34}$$

and for the load estimator:

$$\mathbf{R}_{k_{DIAG}} = \begin{bmatrix} \frac{10\pi}{180} & \frac{10000\pi}{180} & \frac{(2 \cdot 10^5)^2}{2 \cdot 10^7} & \frac{(2 \cdot 10^5)^2}{2 \cdot 10^7} \end{bmatrix}$$
(35)
$$\mathbf{Q}_{k_{DIAG}} = \begin{bmatrix} 10^{-10} & 10^2 & 10^{10} & 10^{14} & 35 \end{bmatrix}$$
(36)

$$\mathbf{Q}_{k_{DIAG}} = \begin{vmatrix} 10^{-10} & 10^2 & 10^{10} & 10^{14} & 35 \end{vmatrix} \tag{36}$$

$$\alpha = 10^{-4} \land \beta = 2 \tag{37}$$

3.2 Load Estimation

In order for the UKF to estimate the loading on the pitch cylinder, the non-linear state transition function has to be augmented to include the load torque as a state, which includes making an assumption of the dynamic behaviour of the unknown stochastic wind load. A reasonable assumption is that the wind load torque is slowly varying compared to the pitch system dynamics and bandwidth as the turbine blade dynamics acts as a low pass filter due to the inherent high inertia.

Therefore, the load torque may be included in the nonlinear state transition function as follows by setting the derivative of the load torque to zero:

$$\begin{bmatrix} \hat{\mathbf{x}} \\ \hat{\tau}_{load} \end{bmatrix} = \begin{bmatrix} \mathbf{f} (\hat{\mathbf{x}}, u) \\ 0 \end{bmatrix}$$
 (38)

An important feature of the load estimation is that it is, and has to be, robust towards variations in internal leakage, such that the load estimation may be included in the leakage estimation algorithm. Therefore, when testing this estimator the leakage coefficient in the simulation model is varied. As described in the previous section the states are scaled to avoid numerical issues in the UKF. As the load torque is included as a state in the UKF, it is scaled by a factor of $\frac{1}{120e3}$, which corresponds to the inverse of the maximum load torque normally experienced at the pitch bearing.

4 Leakage Estimation Using UKF

Normally in a wind turbine pitch system, a velocity sensor is not installed. Therefore, the UKF estimating the leakage needs to be accurate without velocity information, or alternatively a velocity estimator needs to be used. As the leakage flow appears in the continuity equation, which depends on knowing the change in volumes, it is a fair assumption that a velocity estimator is needed to allow the UKF to have enough information about the system. Furthermore, this paper includes the load estimation in the algorithm as a measured disturbance but not a state, where the proposed structure of the leakage estimator is seen in Figure 4. A Super Twisting Sliding Mode (STSM) observer is used to estimate the piston velocity, as it has shown to yield more robust results in similar applications compared to a standard differentiator approach. The STSM algorithm is further explained in the next section.

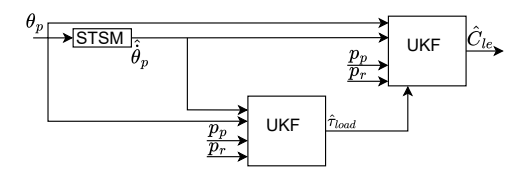


Figure 4: Diagram of the leakage estimation structure using a UKF to estimate the load torque and feeding it to the leakage estimator.

To estimate the leakage coefficient using a UKF, it has to be included as a state in the state transition function. The leakage coefficient is assumed to be slowly varying, as the most common type of leakage change in a system is when the leakage slowly increases

over time. The augmentation of the state transition function is seen in Eq. (39), where \hat{C}_{le} is the estimate of the leakage coefficient of the system:

$$\begin{bmatrix} \hat{\mathbf{x}} \\ \hat{C}_{le} \end{bmatrix} = \begin{bmatrix} \mathbf{f} (\hat{\mathbf{x}}, u) \\ 0 \end{bmatrix}$$
 (39)

Augmenting the system to include the leakage coefficient as a state requires scaling, why the state is scaled by the inverse of the leakage coefficient used for the validated simulation model, which is $C_{le}=1.25$ L/min/hbar.

4.1 Pitch Velocity Estimation

The Super twisting velocity estimator is based on Yuri Shtessel and Levant (2014). The pitch velocity estimation error is defined as:

$$\dot{\hat{\theta}}_p = \dot{\hat{\theta}}_p - \dot{\theta}_p \tag{40}$$

The super twisting algorithm then determines the velocity estimate as:

$$\dot{\hat{\theta}}_p = -h_1 \sqrt{|\tilde{\theta}_p|} sign(\tilde{\theta}_p) + \overline{w}$$
 (41)

$$\dot{\overline{w}} = -h_2 sign(\tilde{\theta}_p) \tag{42}$$

where the constants h_1 and h_2 are chosen as:

$$h_1 = 1.5\sqrt{C_1} h_2 = 1.1C_1$$
 (43)

Where, if C_1 is chosen as a bound on the pitch acceleration, stability of the observer is proven and a sliding mode on $(\tilde{\theta}_p, \dot{\tilde{\theta}}_p) = (0,0)$ exists. Hence, the estimation error $\tilde{\theta}_p$ should ideally be zero. For the pitch system C_1 is chosen as $C_1 = 10 \text{ rad/s}^2$.

As the STSM works as a differentiator, it is quite sensitive to noise. However, it is found that the leakage estimating UKF is able to effectively filter out the noise in the velocity estimate.

5 Simulation Results

The described non-linear model from Section 2 is used as a simulation model depicting a real pitch system. In the simulation model a standard PI controller is designed to control the pitching angle. Furthermore, Gaussian noise is added to the position and pressure signals, to emulate normal working conditions. The position measurement is added a noise of 0.005° standard deviation, and the pressure signals have an added noise of 0.2 bar standard deviation, which both correspond to the noise levels on the physical set-up described in

the following section. The load and leakage estimators are tested using a sample frequency of 1 kHz. During the simulations, the leakage coefficient is gradually increased using a step function to test the load and leakage estimators at different leakage levels ranging from $1\,\mathrm{L/min/hbar}$ to $50\,\mathrm{L/min/hbar}$. In Figure 5 the simulated results of the load estimation can be seen, under a situation where the pitch system is operating under normal load conditions and $17\,\mathrm{m/s}$ wind conditions, which resembles more rough working conditions.

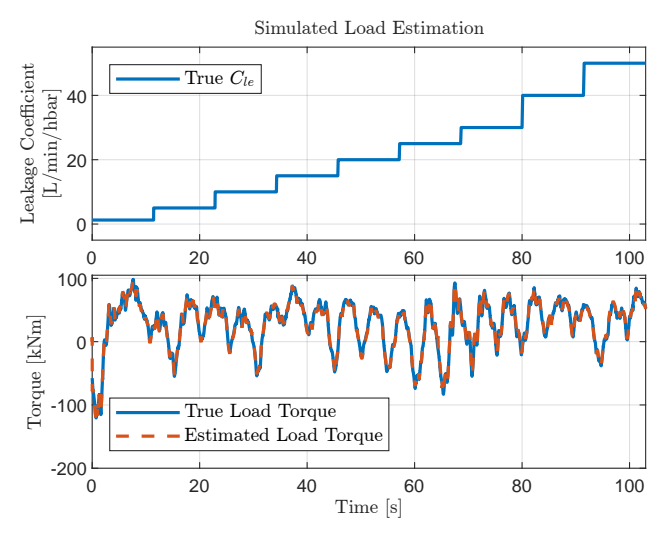


Figure 5: Results of load estimation at different leakages, at a 1 kHz sampling frequency with noise added to the feedbacks.

As shown in the figure, these results are achieved with a leakage fault present which increases in steps over time. This result shows that the UKF is able to accurately estimate the load applied to the pitch cylinder, and that it is robust toward leakage faults. It should be noted that the estimator does not distinguish between the load torque applied by the wind and unmodeled friction dynamics from potential friction faults but estimates the combined unmodeled load torque.

When considering the leakage estimation, the simulation results are shown in Figure 6. From the graphs it may be seen that the leakage estimate using the proposed estimation structure converges for each step in the leakage and estimates the leakage with reasonable accuracy. The initial inaccuracy is due to initialization. It should also be noted that the leakage estimator has a response time of $3\,\mathrm{s}$ to $5\,\mathrm{s}$, which is significantly below normal leakage variations.

To evaluate the robustness of the proposed estimation structure, a series of simulation tests are performed. In these test parameters are changed in the

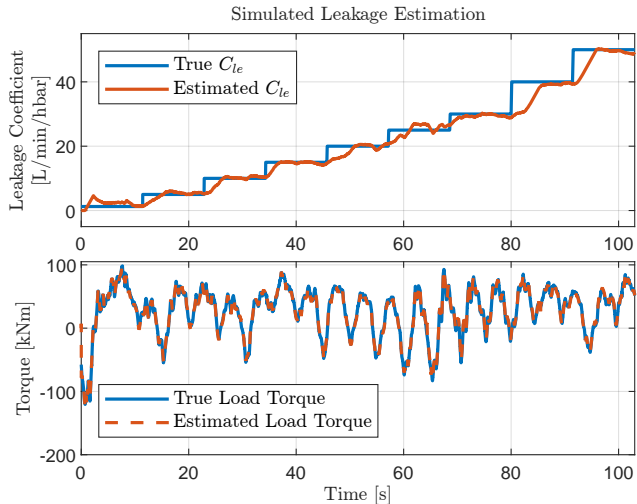


Figure 6: Simulation results for the proposed leakage estimation structure at a 1 kHz sampling frequency.

simulation model but not in the models used in the estimation structure. A single parameter is changed at a time, and each parameter is varied in the range shown in Table 1. All tests are conducted with a constant leakage at $20\,\mathrm{L/min/hbar}$. From this series of simu-

Parameter:	Base Value:	Variation:
ρ	$885\mathrm{kg/m^3}$	$850-900 \text{ kg/m}^3$
eta_p	$10000\mathrm{bar}$	$6\text{-}10~\mathrm{kbar}$
eta_r	$10000\mathrm{bar}$	$8-12~\mathrm{kbar}$
B_v	$175 \mathrm{Nm/(°/s)}$	50-2000 Nm/(°/s)
m_p	$104\mathrm{kg}$	$99\text{-}109~\mathrm{kg}$
J_b	$380\mathrm{kgm}^2$	$190-570 \text{ kgm}^2$

Table 1: Parameter variation range for the leakage estimation robustness tests.

lation tests it is found that only two parameters have an effect on leakage estimation, that being oil density (ρ) and the bulk modulus of the piston side chamber (β_p) . Figure 7 shows the effect of a piston side bulk modulus reduction to 6000 bar, resulting from pressure variations or increased air content in the oil, which is the parameter variation which has the largest effect on the algorithm. However, from the results, it is possible to see that the algorithm is still capable of tracking the leakage accurately.

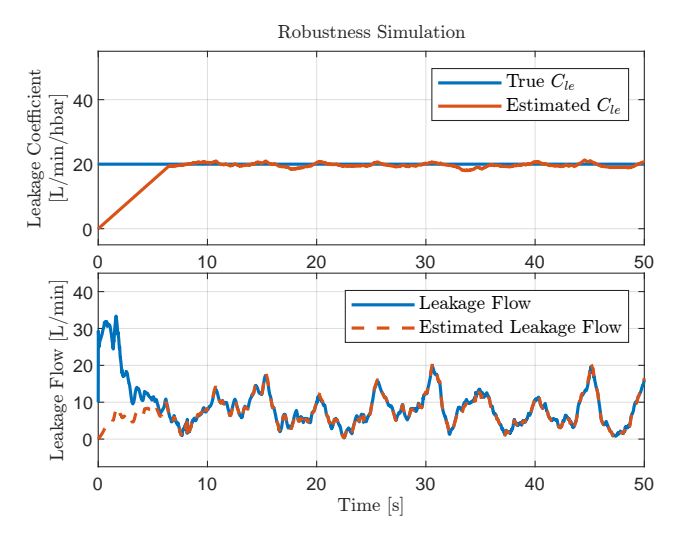


Figure 7: Results of leakage estimation with simulation model $\beta_{0_{p_p}}$ reduced to 6000 bar.

6 Experimental Setup and Results

To test the algorithms in real life, a full scale pitch system designed for a 3MW turbine is utilized. The system is comprised of a pitch bearing, pitch cylinder, proportional valve, valve manifold and corresponding pressure and position sensors as shown in the diagram in Figure 1. The safety system is excluded in the setup, which is a reasonable exclusion, as it is not used under normal operation. Besides the pitch system under investigation the experimental set-up consist of a load cylinder and corresponding valves, and the system HPU including a minor accumulator, which is shared between the two systems. The load cylinder is mounted underneath the bearing and is acting as the load, thus emulating the wind loading and the blade dynamics on the pitch bearing. A picture of the set-up with notation of the main components is shown in Figure 8. To emulate the internal leakage in the pitch system, an extra connection is made between the rod and piston side chambers of the cylinders, in which an on-off valve and a manually adjustable orifice is included. This way the leakage coefficient can be controlled through the manual valve, and the leakage can be enabled and disabled by respectively opening and closing the on-off valve. Unfortunately it has not been possible to fit a flow meter with reasonable resolution to the set-up, and therefore the flow across the leakage emulation valve has been determined via the pressure measurements in the two chambers.

Besides the pressure sensors mounted on the pitch cylinder, pressure sensors are installed to measure supply, tank, and the two pressures in the load cylinder.

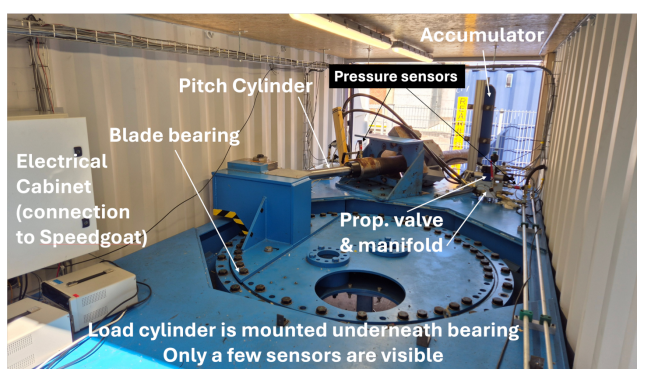


Figure 8: Image of the experimental set-up, with indications of the main components. The position sensor is build into the pitch cylinder, and pressure sensors are connected to each volume. The leakage emulation valve is mounted behind the pitch cylinder in the picture. The speedgoat and HPU is not included in the picture.

All the pressure sensor measurements have a standard deviation of ≈ 0.2 bar and the position sensor measurement has a standard deviation of ≈ 0.5 cm. The algorithms are implemented on a Performance real-time target Speedgoat set-up running Simulink, the pitch controllers, and the UKFs are both running with a sampling frequency of 1kHz. Different tests have been made, and in the following results for respectively 11 m/s and 13 m/s average wind speed are shown, which, respectively, corresponds to just below and above rated wind speed of the turbine. The simulation results from other wind speeds show similar results, but power supply limitations restricts the physical load emulation system to operate below 13 m/s wind speed. The results from the load torque estimation is shown in Figure 9 and Figure 10, whereas the estimated leakage and impact of process noise are shown in Figures 11 and 12, respectively.

From Figure 9 and Figure 10, it is seen that the proposed load estimation algorithm demonstrates solid performance in tracking the actual load dynamics. There is a small offset observed between the true and estimated load values, but despite this the algorithm captures the dynamic behavior very well. It should here be noted that part of the offset may likely be attributable to minor biases in one or more of the pressure measurements, which propagate through the estimation process.

For the adjustment of the Unscented Kalman Filter (UKF), particularly the choice of process noise covariance plays a crucial role in balancing responsiveness and robustness of the estimate. While increasing

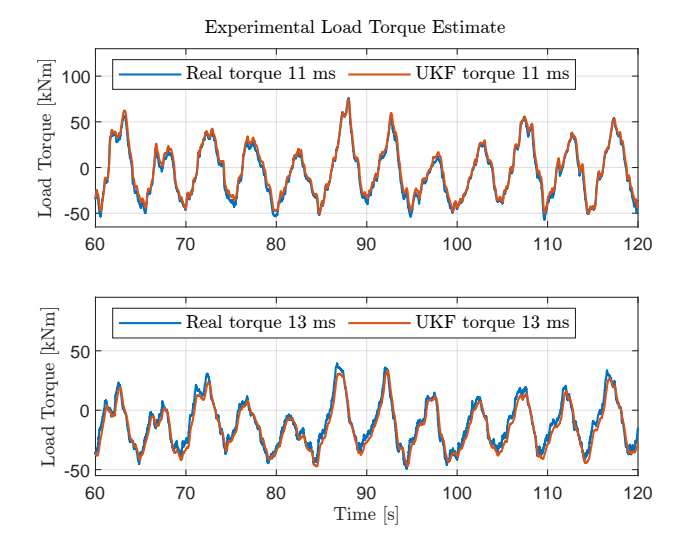


Figure 9: Experimental result of load estimation at 11 and 13 m/s mean wind speed.

the process noise may improve the bandwidth and allow the estimator to follow rapid changes more closely, it also introduces higher sensitivity to measurement noise. Therefore, as the load estimate is subsequently used as input for a leakage estimation algorithm, excessive noise is undesirable and can degrade overall performance. Thus the used values yield a proper compromise. Finally, it should be noted that the algorithm has also been tested with lower sampling frequencies. The results thus show that the algorithm maintains acceptable performance even at reduced sampling frequencies, down to 100 Hz, which makes it suitable for embedded implementations with constrained computational resources or limited sensor update rates.

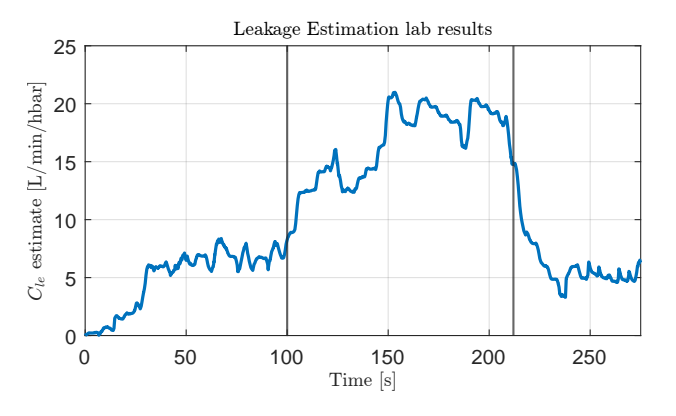


Figure 11: Experimental result of leakage estimation at 11 m/s mean wind speed. The vertical lines represent the time instances where a manual change in the leakage level has been made.

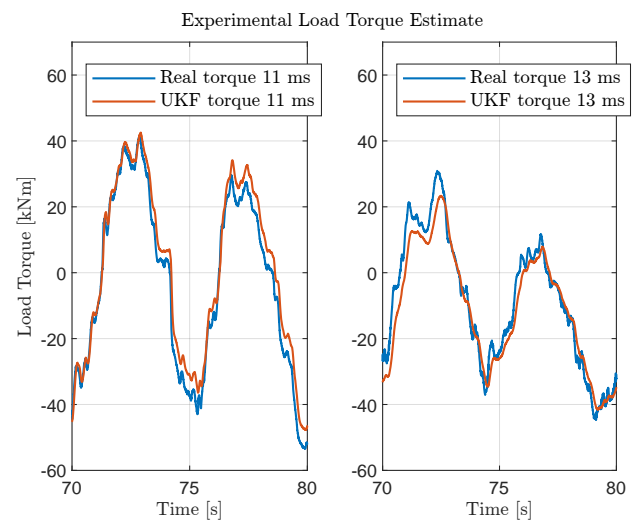


Figure 10: Experimental result of load estimation at 11 and 13 m/s mean wind speed with zoomed view.

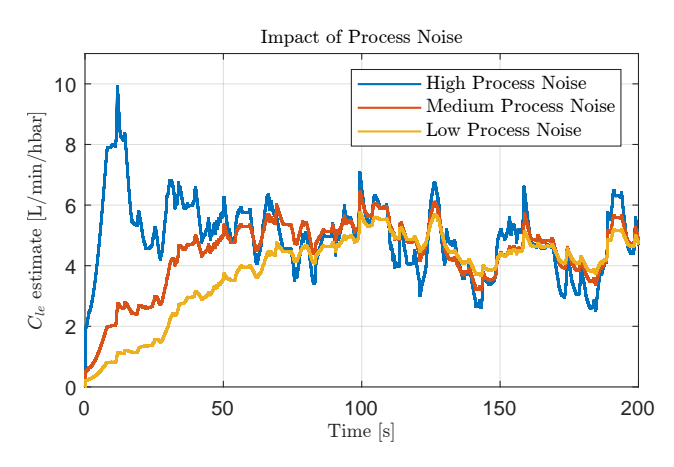


Figure 12: Result of changing process noise parameter in the UKF.

Shifting focus to the leakage estimation experiments, Figure 11 shows the result for the 11 m/s test case. The leakage estimation algorithm was evaluated through a 300-second time span, where the first and last 100 seconds of the leakage estimate test corresponds to the internal leakage across the valve, while in the middle period the leakage flow in the cylinder was increased to emulate a change in leakage coefficient. From the graph it can be seen that the estimator successfully tracked these changes, with the estimated leakage settling at consistent values during repeated low leakage conditions, and at a distinct higher level during the middle phase. Results with similar characteristics and

convergence was seen for other wind velocities.

As for the load estimator algorithm, the adjustment of the process noise parameter of the UKF directly influences the responsiveness of the estimator. A lower process noise leads to a slower-varying estimate with reduced sensitivity to measurement fluctuations, while a higher process noise results in a more responsive estimate. However, tests conducted at a constant leakage level show that the mean estimated leakage remains largely unaffected by the choice of process noise. The differences are therefore primarily observed in the settling time and the magnitude of oscillations in the transient response, making the algorithm fairly robust to real process noise variations, as leakage is typically a slow varying phenomenon, where it is the static value that is of interest.

7 Conclusion

As described in the introduction, leakage is a significant failure mode in hydraulic pitch systems, but the methods considered in literature for leakage estimation in hydraulic systems have typically relied on constant or known load forces. The focus of the current study has therefore been on the development and validation of a load and leakage estimation method for hydraulic pitch systems in wind turbines using an Unscented Kalman Filter. The method addresses the challenge of unknown and stochastic wind loads by incorporating a load estimation algorithm for predicting the load torque action on the blade bearing and hence the pitch cylinder. Simulation results confirmed the robustness of the approach to parameter variations and noise, while experimental validation on a full-scale pitch system demonstrated accurate leakage and load torque estimation. The findings thus suggest that the proposed method can be used to enhance the reliability and efficiency of wind turbine operations by enabling real-time condition monitoring and early fault detection of leakage faults, while also being applicable to other types of hydraulic systems with unknown load conditions.

References

- Choux, M., Tyapin, I., and Hovland, G. Leakage-detection in blade pitch control systems for wind turbines. In *Proceedings Annual Reliability and Maintainability Symposium*. 2012. doi:10.1109/RAMS.2012.6175515.
- Dallabona, A., Blanke, M., and Papageorgiou, D. Friction Estimation for Condition Monitoring of Wind Turbine Hydraulic Pitch System. In *IFAC*-

- PapersOnLine, volume 58. Elsevier B.V., pages 598–603, 2024. doi:10.1016/j.ifacol.2024.07.284.
- Dallabona, A., Blanke, M., Pedersen, H. C., and Papageorgiou, D. Fault diagnosis and prognosis capabilities for wind turbine hydraulic pitch systems. *Mechanical Systems and Signal Processing*, 2025. 224:111941. doi:10.1016/j.ymssp.2024.111941.
- Julier, S. J. and Uhlmann, J. K. New extension of the Kalman filter to nonlinear systems. In Signal Processing, Sensor Fusion, and Target Recognition VI, volume 3068. International Society for Optics and Photonics, SPIE, pages 182 193, 1997. doi:10.1117/12.280797.
- Lu, B., Li, Y., Wu, X., and Yang, Z. A review of recent advances in wind turbine condition monitoring and fault diagnosis. In 2009 IEEE Power Electronics and Machines in Wind Applications, PEMWA 2009. 2009. doi:10.1109/PEMWA.2009.5208325.
- Ma, R., Zhao, H., Wang, K., Zhang, R., Hua, Y., Jiang, B., Tian, F., Ruan, Z., Wang, H., and Huang, L. Leakage Fault Diagnosis of Lifting and Lowering Hydraulic System of Wing-Assisted Ships Based on WPT-SVM. *Journal of Marine Science and Engi*neering, 2023. 11(1). doi:10.3390/jmse11010027.
- Márton, L., Fodor, S., and Sepehri, N. A practical method for friction identification in hydraulic actuators. *Mechatronics*, 2011. 21(1). doi:10.1016/j.mechatronics.2010.08.010.
- Na, Q., Feng, G., and Tian, T. Real-Time Leak Detection in High Frequency Hydraulic Cylinder Based on Intelligent Control. Wireless Communications and Mobile Computing, 2022. 2022. doi:10.1155/2022/4753328.
- Padman, P., Xu, J., Vanni, F., Echavarria, E., and Wilkinson, M. The Effect of Pitch System Reliability on Wind Power Generation's Levelized Cost of Energy. White paper, Moog Industrial Solutions and DNV GL, 2016. Wind Europe 2016 presentation.
- Palanimuthu, K. and Joo, Y. H. Reliability improvement of the large-scale wind turbines with actuator faults using a robust fault-tolerant synergetic pitch control. *Renewable Energy*, 2023. 217. doi:10.1016/j.renene.2023.119164.
- Shields, M., Beiter, P., Nunemaker, J., Cooperman, A., and Duffy, P. Impacts of turbine and plant upsizing on the levelized cost of energy for offshore wind. *Applied Energy*, 2021. 298. doi:10.1016/j.apenergy.2021.117189.

- Simon, D. Optimal state estimation: Kalman, H infinity, and nonlinear approaches. John Wiley & Sons, 2006. doi:10.1002/0470045345.
- Van Der Merwe, R. and Wan, E. A. The square-root unscented kalman filter for state and parameter-estimation. In 2001 IEEE international conference on acoustics, speech, and signal processing. Proceedings (Cat. No. 01CH37221), volume 6. IEEE, pages 3461–3464, 2001. doi:10.1109/ICASSP.2001.940586.
- Walgern, J., Fischer, K., Hentschel, P., and Kolios, A. Reliability of electrical and hydraulic pitch systems in wind turbines based on field-data analysis. *Energy Reports*, 2023. 9. doi:10.1016/j.egyr.2023.02.007.
- Wan, E. A. and van der Merwe, R. The Unscented

- Kalman Filter, chapter 7, pages 221–280. John Wiley & Sons, Ltd, 2001. doi:10.1002/0471221546.ch7.
- Wu, X., Li, Y., Li, F., Yang, Z., and Teng, W. Adaptive estimation-based leakage detection for a wind turbine hydraulic pitching system. *IEEE/ASME Transactions on Mechatronics*, 2012. 17(5). doi:10.1109/TMECH.2011.2142400.
- Yuri Shtessel, L. F., Christopher Edwards and Levant, A. *Sliding Mode Control and Observation*. Birkhäuser, 2014. doi:10.1007/978-0-8176-4893-0.
- Zhao, X., Zhang, S., Zhou, C., Hu, Z., Li, R., and Jiang, J. Experimental study of hydraulic cylinder leakage and fault feature extraction based on wavelet packet analysis. *Computers and Fluids*, 2015. 106. doi:10.1016/j.compfluid.2014.09.034.

